Journal of Experimental Botany, Vol. 71, No. 3 pp. 1053–1066, 2020
doi:10.1093/jxb/erz455 Advance Access Publication October 18, 2019

RESEARCH PAPER

Redox homeostasis in the growth zone of the rice leaf plays a key role in cold tolerance

Ayelén Gázquez[1,2], Hamada AbdElgawad[1,3], Geert Baggerman[4,5,6], Geert Van Raemdonck[4], Han Asard[1], Santiago Javier Maiale[2], Andrés Alberto Rodríguez[2], and Gerrit T.S. Beemster[1,*]

[1] Laboratory for Integrated Molecular Plant Physiology Research (IMPRES), Department of Biology, University of Antwerp, Groenenborgerlaan 171, 2020 Antwerp, Belgium
[2] Laboratorio de Fisiología de Estrés Abiótico en Plantas, Unidad de Biotecnología 1, IIB-INTECH - CONICET - UNSAM, Chascomús, Argentina
[3] Department of Botany and Microbiology, Science Faculty, Beni-Suef University, Beni-Suef 62511, Egypt
[4] Centre for Proteomics (CFP) Core Facility, University of Antwerp, Groenenborgerlaan 171, 2020 Antwerp, Belgium
[5] Systemic Physiological & Ecotoxicological Research (SPHERE), Department of Biology, University of Antwerp, Groenenborgerlaan 171, 2020 Antwerp, Belgium
[6] Flemish Institute for Technological Research (VITO), Mol, Belgium

* Correspondence: gerrit.beemster@uantwerpen.be

Received 3 September 2019; Editorial decision 26 September 2019; Accepted 27 September 2019

Editor: Christine Foyer, University of Birmingham, UK

Abstract

We analysed the cellular and molecular changes in the leaf growth zone of tolerant and sensitive rice varieties in response to suboptimal temperatures. Cold reduced the final leaf length by 35% and 51% in tolerant and sensitive varieties, respectively. Tolerant lines exhibited a smaller reduction of the leaf elongation rate and greater compensation by an increased duration of leaf growth. Kinematic analysis showed that cold reduced cell production in the meristem and the expansion rate in the elongation zone, but the latter was compensated for by a doubling of the duration of cell expansion. We performed iTRAQ proteome analysis on proliferating and expanding parts of the leaf growth zone. We identified 559 and 542 proteins, of which 163 and 210 were differentially expressed between zones, and 96 and 68 between treatments, in the tolerant and sensitive lines, respectively. The categories protein biosynthesis and redox homeostasis were significantly overrepresented in the up-regulated proteins. We therefore measured redox metabolites and enzyme activities in the leaf growth zone, demonstrating that tolerance of rice lines to suboptimal temperatures correlates with the ability to up-regulate enzymatic antioxidants in the meristem and non-enzymatic antioxidants in the elongation zone.

Keywords: iTRAQ, kinematic analysis, leaf growth, redox, rice, suboptimal temperature stress.

Introduction

An important limitation to yield in rice is sensitivity to suboptimal temperatures during the seedling stage (Allen and Ort, 2001; Quintero, 2009; Laurance *et al.*, 2014; FAO, 2016; Wang *et al.*, 2016). Suboptimal temperatures are defined as those between the minimum and the optimum temperature for growth: for rice, between 12–13 °C and 25–30 °C, respectively. Chilling temperatures range from 0 °C to the minimum temperature for growth (Yoshida, 1981; Menéndez *et al.*, 2013).

Unlike chilling, which occurs only occasionally during the rice growth season, suboptimal temperatures persist for long periods and have a significantly negative impact on rice yield (Allen and Ort, 2001; Quintero, 2009; Clayton and Neves, 2011; Wang *et al.*, 2016). Previously, we found contrasting responses to suboptimal temperatures in terms of the growth and physiology of rice seedlings in a group of eight cultivars (Gazquez *et al.*, 2015). The study classified these cultivars as tolerant or sensitive based on the inhibition of seedling growth. This was correlated with a reduction of active chlorophyll and photosystem II performance in the sensitive cultivars, whereas the tolerant cultivars had a stronger reduction of stomatal conductance and an increase of water use efficiency. In agreement with these findings, our recent transcriptome study of two of the contrasting cultivars demonstrated that photosystem II genes were down-regulated in the sensitive cultivar (Gazquez *et al.*, 2018). Together with biochemical and physiological analyses, our results showed that the maintenance of photosynthetic capacity is crucial for cold tolerance in rice.

Other reports have shown that antioxidant metabolites and enzymes also contribute to cold tolerance (Kuk *et al.*, 2003; Grohs *et al.*, 2016) and correlate with growth performance (Chakraborty and Bhattacharjee, 2015). Cells are the building blocks of the plant body and the regulatory units that integrate locally perceived chemical and physiological signals by genetically encoded molecular regulatory networks that ultimately control the growth process (Gonzalez *et al.*, 2012; Kalve *et al.*, 2014; Czesnick and Lenhard, 2015). Variation in cell division and expansion parameters explain differences in organ size between species (Gázquez and Beemster, 2017) and the differential growth response of varieties with contrasting tolerance to stress conditions (Avramova *et al.*, 2017). However, it remains unknown how redox regulation in the growth zone affects cellular growth processes and cold tolerance.

Adverse environmental conditions affect physiological processes by altering gene expression, resulting in changes at the proteome level (Kosová *et al.*, 2011; Hakeem *et al.*, 2012; Barkla *et al.*, 2013). A few studies have analysed the proteome of rice leaves at the seedling stage subjected to suboptimal temperatures (Cui *et al.*, 2005; Gammulla *et al.*, 2011; Neilson *et al.*, 2011). However, in order to identify specific changes related to the inhibition of cell division and expansion, it is necessary to sample proliferating and expanding tissues. Other proteome studies compared these developmental zones in maize leaves (Majeran *et al.*, 2010; Facette *et al.*, 2013; Ponnala *et al.*, 2014) and roots (Marcon *et al.*, 2015), both under standard conditions and to study the effect of drought stress (Avramova, 2016).

Understanding how cell division and expansion are affected by stress and the underlying molecular changes enables the identification of tolerance mechanisms that could be used in breeding programs. Therefore, in this study we subjected three tolerant and three sensitive rice cultivars (Gazquez *et al.*, 2015) to optimal (24/28 °C night/day) and suboptimal (13/21 °C night/day) temperatures and performed a kinematic analysis of the fourth leaf and a proteome analysis on samples of the meristem and the elongation zone of the leaf of two contrasting cultivars. Subsequent metabolite and biochemical analyses investigating antioxidant regulation in the leaf growth zone allowed us to relate cellular responses to antioxidant capacity.

Materials and methods

Plant material and growth conditions

Rice (*Oryza sativa*) seeds of the tolerant cultivars Koshihikari, CT-6742-10-10-1, and General Rossi and the sensitive varieties IR50, IR24, and Honezhaosen were provided by the Rice Breeding Program of the Universidad Nacional de La Plata, Argentina (Gazquez *et al.*, 2015). Seeds were germinated according to Gazquez *et al.* (2015). Seedlings were transplanted to peat potting medium (Jiffy, The Netherlands) in 1.6 litre pots 13 cm high and 12.7 cm in diameter, and grown in a growth chamber (Conviron, Adaptis A1000) under controlled conditions with a 12 h photoperiod, 350 µmol photons m^{-2} s^{-1} photosynthetically active radiation, and 80% humidity. Temperatures for control conditions were 28/24 °C day/night. When the third leaf (Yoshida, 1981) emerged, plants were exposed to suboptimal temperatures of 21/13 °C day/night.

Two days after the emergence of the fourth leaf, two pools of 10 Koshihikari and IR50 plants were randomly selected from the control and suboptimal temperature treatments and harvested for protein extraction and redox state measurements. The growth zone of the fourth leaf of each plant was cut into five segments based on the results of kinematic analysis for the control and suboptimal temperature treatments, starting from the base of the leaf: meristem (4 mm for the control and 3 mm for the suboptimal temperature treatment), transition zone (3 mm and 2 mm), elongation zone (18 mm and 10 mm), transition zone 2 (5 mm and 3 mm), and mature zone (20 mm and 20 mm) (see Supplementary Fig. S1 at *JXB* online). Samples were immediately frozen in liquid nitrogen and stored at –80 °C for further analyses.

Growth and kinematic analysis

To determine the leaf elongation, rate the length of the fourth leaf (Yoshida, 1981) was measured daily with a ruler, using the top of the soil as a reference point. Measurements were carried out on the fourth leaf of 23 plants per cultivar/treatment, 2 h after the start of the photoperiod, from emergence until the final length was reached. The leaf elongation rate was calculated as the difference in leaf length divided by the time interval between successive measurements. Kinematic analysis was performed on the fourth leaf of five plants of each cultivar/treatment on the second day after emergence from the whorl of older leaves (i.e. during steady-state growth) following a previously described protocol (Rymen *et al.*, 2010; Pettkó-Szandtner *et al.*, 2015). Briefly, the fourth leaf was harvested by removing the older leaves with forceps and a scalpel. Imprints of the abaxial epidermis of the basal 4 cm (for controls) or 5 cm (for suboptimal temperature conditions) of the leaf were made with nail varnish and transferred to microscope slides by means of cellophane tape. The first 2 cm from the basal part of the same leaf that was used for the imprints was placed in 3:1 v/v absolute ethanol:acetic acid for fixation and clearing. Samples were kept at 4 °C for a period ranging from 24 h up to several weeks before use. They were washed for 20 min in buffer containing 0.05 M Tris–HCl (pH 7.0) and 0.5% Triton X-100, and incubated with 1 µg ml^{-1} DAPI in wash buffer for 5–7 min. Nuclei were observed with a fluorescence microscope (AxioScope A1, Axiocam ICm1, Zeiss) at ×20 magnification. The length of meristematic zone of the leaves was determined by locating the most distal mitosis in the abaxial epidermis relative to the base of the leaf (Pettkó-Szandtner *et al.*, 2015). The length of cells next to stomata files (Luo *et al.*, 2012) was measured at 1 mm intervals on the imprints of the leaf by bright-field microscopy (AxioScope A1, Axiocam ICm1; Zeiss) at ×40 for the meristematic zone and ×20 for the elongating and mature cells, using the online measurement module in Axiovision (vs 4.8, Zeiss) software. The raw cell-length data from individual leaves were smoothed using the Locpoly function of the Kern Smooth package (Wand and Jones, 1995) for the R statistical package (R Foundation for Statistical Computing). Indirect kinematic analysis to calculate cell division and expansion parameters was performed as described by Fiorani and Beemster (2006). All parameters were averaged between leaves and used for calculations of cell division and expansion parameters.

Thermal time calculation

Thermal time, expressed as growing degree days (GGD), for each treatment and cultivar was calculated by integration of leaf temperatures over time (Bonhomme, 2000):

$$GDD = \frac{(T_{Max} - T_{Base}) * h_{T_{Max}} + (T_{Min} - T_{Base}) * h_{T_{Min}}}{24}$$

Where T_{Max} is the daily maximum air temperature; T_{Min} is the daily minimum air temperature; T_{Base} is the temperature below which the leaf does not grow; $h_{T_{Max}}$ is the number of hours of light; and $h_{T_{Min}}$ is the number of hours of darkness. T_{Base} was set to 10 °C (Lee, 1979; Gao *et al.*, 1992; Sánchez *et al.*, 2014), and $h_{T_{Max}}$ and $h_{T_{Min}}$were 12 h for all treatments. Therefore, equation (1) could be simplified as follows:

$$GDD = \left[\left(\frac{T_{Max} - T_{Min}}{2}\right) - 10\right]$$

Protein extraction and digestion

Sample pools labelled with an 8-plex iTRAQ kit were prepared as follows. Proteins were extracted according to Méchin *et al.* (2007) with minor modifications. Samples were ground in liquid nitrogen, and 1.8 ml 0.07% 2-β-mercaptoethanol and 10% trichloroacetic acid in cold acetone were added. After overnight incubation at –20 °C, samples were centrifuged for 30 min at 10 000 *g* and 4 °C, and the pellet was washed twice in 100% acetone. The pellets were then dissolved in 0.5 M triethylammonium bicarbonate (TEAB). Protein concentrations were determined by using a Pierce BCA Protein Assay Kit (Thermo Fisher Scientific) and a NanoDrop 2000 spectrophotometer (Thermo Fisher Scientific). From each sample, 100 µg of protein was denatured and reduced using reagents supplied with the iTRAQ labelling kit (AB Sciex) in 20 µl 100 mM TEAB and incubated at 60 °C for 1 h. After cysteine blocking with Cysteine Blocking Reagent for 10 min in the dark, six volumes of cold acetone were added and samples were incubated overnight at –20 °C. After centrifugation for 10 min at 10 000 *g* and 4 °C, the proteins were dissolved in 20 µl of 100 mM TEAB and digested with MS-grade Trypsin Gold (enzyme:protein ratio = 1:10; Promega) overnight at 37 °C. The next day, samples were desalted with Pierce C18 Spin Columns following the manufacturer's instructions (Thermo Fisher Scientific).

iTRAQ protein labelling

An iTRAQ Reagents 8-plex kit (AB Sciex) was used for the labelling. The iTRAQ labels were dissolved in 50 µl isopropanol. Digested peptides were labelled with the iTRAQ reagents and incubated for 2 h at ambient temperature. Pooled samples were prepared with equimolar peptide concentration ratios.

Nano-reversed-phase liquid chromatography and mass spectrometric data analyses

The iTRAQ-labelled samples were analysed by LC-tandem MS in a data dependent acquisition (DDA) set-up. Reversed-phase (RP) chromatography was performed on an Easy-nLC system (Thermo Scientific). An Acclaim PepMap RP-C18 trap column (3 µm, 100 Å, 75 µm×20 mm) and an Acclaim PepMap RP-C18 analytical column (2 µm, 100 Å, 50 µm×150 mm) were used. A 1 µg aliquot of pooled iTRAQ-labelled peptide dissolved in 10 µl of mobile phase A (2% ACN and 0.1% formic acid) was loaded. A linear gradient of mobile phase B (98% ACN and 0.1% formic acid) from 2% to 40% in 300 min was used at a flow rate of 400 nl min^{-1}.

Three biological replicates (each comprising 10 pooled leaf sections) of each combination of cultivars (Koshihikari and IR50), zones (meristem and elongation zone), and treatments (control and suboptimal temperature) were analysed in three 8-plex iTRAQ pools (eight different biological samples in total; see Supplementary Table S1). The nano-LC was coupled online with a Q-Exactive Plus Hybrid Quadrupole-Orbitrap mass spectrometer (Thermo Scientific) running in MS/MS mode, where a full scan spectrum (350–2000 m/z) was done. The top five most abundant peaks in each full scan were selected for fragmentation in a DDA set-up. The normalized collision energy used was 32% in collision-induced dissociation with a dynamic exclusion time of 30 seconds. Fragmentation was set to high-energy collision-activated dissociation scans.

Proteome data analysis

Proteome Discoverer software (version 1.3.0.339, Thermo Scientific) was used to perform database searches against the UniProt *Oryza sativa* subsp. *indica* (39946) and UniProt *Oryza sativa* subsp. *japonica* (39947) databases using SEQUEST and Mascot (Matrix Science) algorithms. Mass spectrum range was set at 300–8000 Da with precursor mass tolerance of 10 ppm, fragment mass tolerance of 0.02 Da, trypsin as digesting enzyme, and allowing two missed cleavages. iTRAQ 8-plex (N-terminus and lysine residues) and Methylthio (C) were defined as fixed modifications, while oxidation (M) and iTRAQ 8-plex (tyrosine residues) were selected as variable modifications. The results were filtered for confident peptide-to-spectrum matches (PSMs) based on a non-concatenated target decoy database. The decoy database is a reversed version of the target database. Only first-ranked peptides with a global false discovery rate (FDR) smaller than 1% were included in the results. All sequences and reporter ion intensities of the PSMs that matched the confidence requirements were exported in CSV format to a spreadsheet for further data analysis (Supplementary Table S2). Data from the three iTRAQ sample pools were normalized with the CONSTANd method (Maes *et al.*, 2016) so peptides could be compared within and between the multiplex experiments without the need of a reference sample (Supplementary Table S3). For statistical and bioinformatics analysis, as well as visualization, Perseus 1.5.5.3 open software (Tyanova *et al.*, 2016) was used. Peptides listed with multiple accessions or no identification were removed and only sequences yielding single protein identifications were kept for further analysis to increase the confidence of the quantification. Relative peptide abundances were log_2-transformed and missing values were replaced from normal distribution with default settings, width of 0.3, and down shift of 1.8 (Lazar *et al.*, 2016; Tyanova *et al.*, 2016). IR50 data were further analysed based on the UniProt *Oryza sativa* subsp. *indica* (39946) database, and Koshihikari data based on the UniProt *Oryza sativa* subsp. *japonica* (39947) database. All peptides matching with the same protein were averaged, and a two-way ANOVA was performed in each cultivar, using treatment and zone as factors, with the built-in ANOVA functions of Perseus software. FDR was applied as a multiple testing correction, and a post-hoc Fisher test was applied when the interaction of factors showed a *P*-value <0.05 (Supplementary Table S4).

Proteins with uncorrected *P*-values <0.05 in the two-way ANOVAs were *Z*-score normalized and clustered using *K*-means with Euclidean distance and average linkage in Perseus software. An enrichment analysis was done for each cluster using DAVID (Huang *et al.*, 2009*a*, *b*) with the UniProt KB identifiers. In the case of IR50 the analysis was done with *japonica* identifiers obtained from the Gramene (http://gramene.org/) database (Youens-Clark *et al.*, 2011) (Supplementary Table S4). The annotation was made with UniProt keywords (UP_KEYWORDS), Gene Ontology (GO) biological process (GOTERM_BP_DIRECT), GO cellular component (GOTERM_CC_DIRECT), GO molecular function (GOTERM_MF_DIRECT), and KEGG pathways (KEGG_PATHWAYS). The enrichment required a minimum of two proteins for a term to be considered, EASE <0.05, Bonferroni <0.1 for multiple testing correction, and *Oryza sativa* subsp. *japonica* as background.

Redox state analyses

For all combinations of cultivar (Koshihikari and IR50), treatment (control and suboptimal temperature), and segment (meristem and elongation zone), three pools (each of 10 plants; Supplementary Fig. S1) of 15–100 mg were homogenized with different extraction buffers/solvents, depending on the target analysis. Homogenates were centrifuged (17 530 *g*, 4 °C, 30 min). The extraction and measurement of each metabolite/enzyme were performed on the same day. Supernatants were used for the following analyses.

H_2O_2

Samples were homogenized in 1 ml of 5% (w/v) TCA using a MagNALyser (Roche, Roche, Vilvoorde, Belgium). The H_2O_2 concentration was measured by monitoring the peroxide-mediated oxidation of Fe^{2+}, followed by reaction of Fe^{3+}, with xylenol orange according to the FOX1 method (Bellincampi *et al.*, 2000). After 45 min incubation, the Fe^{3+}–xylenol orange complex was measured at 600 nm. Standard curves were obtained by adding known H_2O_2 concentrations to the xylenol orange reagent. The specificity of the reaction for H_2O_2 was ascertained by eliminating H_2O_2 with catalase. Data were normalized and expressed as μM H_2O_2 per gram of fresh weight (FW) tissue.

Lipid peroxidation marker (malondialdehyde)

Malondialdehyde (MDA) was extracted from homogenized leaves in 80% ethanol (MagNALyser; 1 min, 7000 rpm) and its level was measured by using the thiobarbituric acid (TBA) assay (Hodges *et al.*, 1999). A 25 μl measure of the supernatant was heated with 25 μl of 0.5% (w/v) TBA in 20% (w/v) trichloroacetic acid at 95 °C for 1 h. Samples were centrifuged (17 530 *g*, 4 °C, 30 min), and the absorbance was measured at 440, 532, and 600 nm in a 96-well microplate (Synergy H1, BioTek). Data were expressed as MDA equivalents (nmol g FW^{-1}) according to Du and Bramlage (1992).

Non-enzymatic antioxidant capacity

Total non-enzymatic antioxidant capacity was determined in extracts prepared in 80% ethanol (v/v), and quantified by the ferric reducing ability of plasma (FRAP) assay (Benzie and Strain, 1996). A 25 μl measure of the supernatant was mixed with an equal volume of 0.3 M acetate buffer (pH 3.6), containing 10 mM 2,4,5-Tris-(2-pyridyl)-*s*-triazine and 200 mM $FeCl_3$. The absorbance was measured at 600 nm in a microplate reader (Synergy H1, BioTeK); 6-hydroxy-2,5,7,8-tetramethylchroman-2-carboxylic acid (Trolox) was used for the standard curve. Data were expressed as Trolox equivalents (μM g FW^{-1}).

Polyphenol concentration

Polyphenols were extracted in 80% ethanol and their concentration was determined using the Folin–Ciocalteu reagent (Zhang *et al.*, 2006). Absorbance was measured at 765 nm in a 96-well microplate (Synergy H1, BioTeK). Gallic acid (GA) was used to prepare standard curves. Data were expressed as GA equivalents (mg g FW^{-1}).

Ascorbate and glutathione concentrations

Frozen plant tissue was extracted in 1 ml ice-cold 6% (w/v) *meta*-phosphoric acid, and ascorbate (ASC) and glutathione (GSH) levels were determined by HPLC (Potters *et al.*, 2004). Antioxidants were separated on an RP column (100×4.6 mm Polaris C_{18}-A, 3 mm particle size; 40 °C) with an isocratic flow rate of 1 ml min^{-1} of elution buffer (2 mM KCl, pH 2.5 adjusted with *O*-phosphoric acid). The components were quantified using a custom-made electrochemical detector, and the purity and identity of the peaks was confirmed using an in-line diode-array detector (SPD-M10AVP, Shimadzu). ASC was measured at 242 nm and GSH at 196 nm. Chromatogram analysis was performed with the Class VP 5.0 software package (Shimadzu). The total reduced antioxidant concentration was determined after reduction with 0.04 M DTT.

Enzyme extraction and enzyme activity assays

Samples were homogenized in 500 μl potassium phosphate buffer (0.05 M, pH 7.0) containing 2% w/v polyvinyl pyrrolidone, EDTA (0.4 mM), and phenylmethylsulfonyl fluoride (0.2 mM), using a MagNALyser (Roche). Peroxidase activity was measured by monitoring the production of purpurogallin at 430 nm (Kumar and Khan, 1982). Catalase activity was calculated from the decrease in H_2O_2 concentration measured at 240 nm (Aebi, 1984). Inhibition of nitroblue tetrazolium reduction at 550 nm was used to assay superoxide dismutase (SOD) activity (Dhindsa *et al.*, 1981). The activities of ascorbate peroxidase (APX), glutathione reductase, glutathione peroxidase, monodehydroascorbate reductase, and dehydroascorbate reductase were assayed according to Murshed *et al.* (2008). Glutaredoxin activity was measured by monitoring the NADPH-dependent reduction of GSH (Lundberg *et al.*, 2001). Thioredoxin activity was indirectly measured as the ability to reduce NADP-malate dehydrogenase, whose activity was measured as the capacity of reducing NADPH (Wolosiuk *et al.* 1979). Thioredoxin was reduced with DTT before the assay.

Soluble protein content

Soluble protein was determined following the Lowry method (Lowry *et al.*, 1951) with BSA as a standard.

Statistical analysis

Statistical analysis of kinematics data was performed using ANOVA and post-hoc Tukey tests with Infostat (Di Rienzo *et al.*, 2016). Redox metabolites and enzyme activities were subjected to a three-way ANOVA with the factors cultivar, treatment, and zone, and interactions of these factors, with Infostat. A post-hoc Duncan test was done when a positive interaction was found.

Results

Leaf growth analysis

We studied the leaf growth zone of seedlings of six rice cultivars with contrasting tolerance subjected to suboptimal and optimal temperatures. We assessed the overall effect of suboptimal temperatures on leaf growth by quantifying the effect on final leaf length. Across all cultivars (Supplementary Table S5), suboptimal temperatures reduced the final length of the fourth leaf by on average 41% (Fig. 1, Table 1). Final leaf length is determined by the rate of leaf elongation and the duration of elongation. Both parameters were affected by suboptimal temperatures: on average, leaf elongation rates were reduced by 76%, whereas the duration of leaf growth was increased by 98%, largely compensating for the reduced elongation rate. Next, we determined the cellular basis of the reduced elongation rates by kinematic analysis, based on measurements of the cell length profile along the growth zone (Supplementary Fig. S2) and the length of the meristem. The inhibition of leaf elongation in response to suboptimal temperatures was explained by a reduction of 67% in the cell production rate and a reduction of 25% in mature cell length (Table 1). The reduction in cell production, in turn, was due to a 55% reduction of the cell division rate and a 25% reduction in the number of dividing cells, reflected by a 20% reduction in meristem size. The 35% reduction in the length of mature cells was due to a 68% lower relative expansion rate, which was partly compensated by a doubling of the duration of cell expansion. Due to the reduced cell length, the length of the elongation zone was also smaller (–28%), whereas the number of expanding cells was not affected.

A comparison of the lines with contrasting tolerance shows that tolerant varieties generally have a greater final leaf length and leaf elongation rate than sensitive lines, which in turn was due to higher cell production, primarily related to a larger meristem (Table 1). In response to suboptimal temperatures, the final leaf length of the sensitive cultivars was reduced by

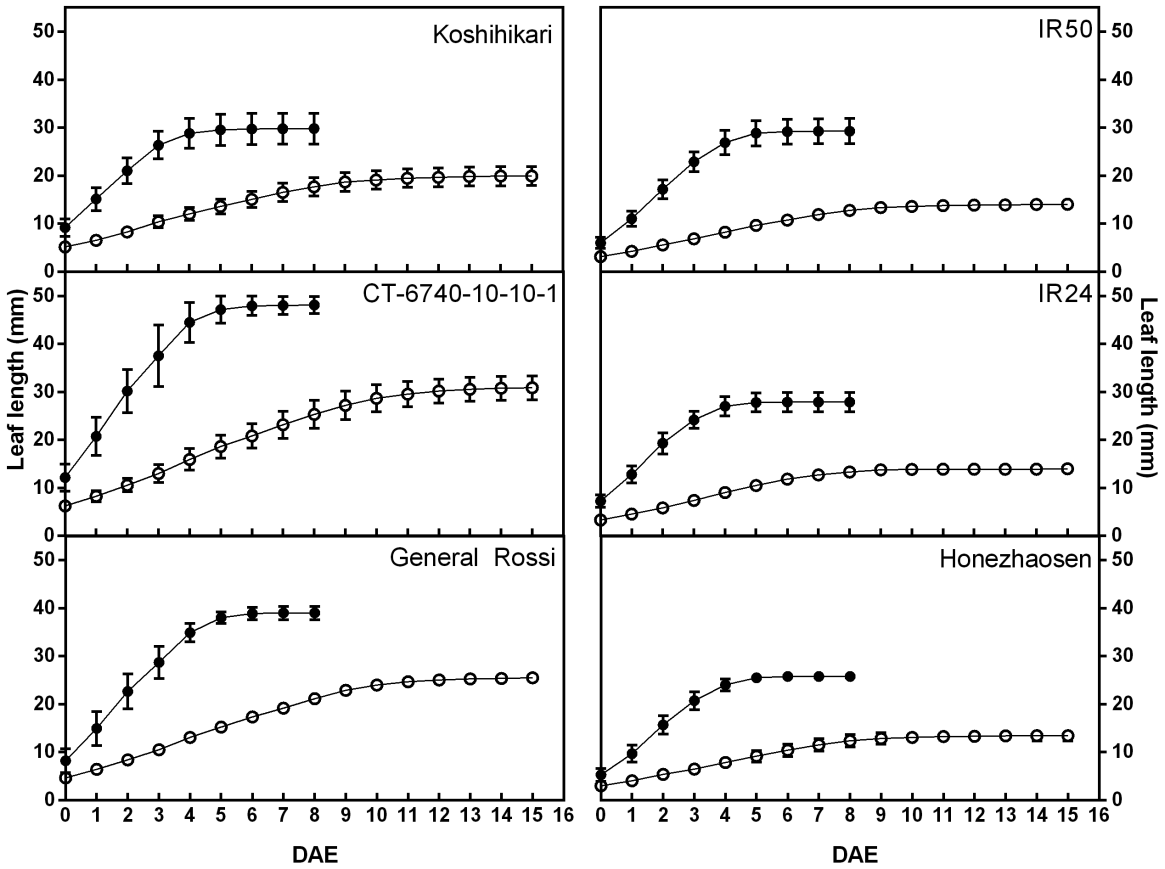

Fig. 1. Effect of suboptimal temperatures on the leaf length of rice cultivars with contrasting tolerance. Koshihikari, CT-6742-10-10-1, and General Rossi are tolerant cultivars, and IR50, IR24, and Honezhaosen are sensitive cultivars. DAE, Days after emergence of the leaf. Values are mean ±SD (n=23).

Table 1. Kinematic analysis of the effect of suboptimal temperatures on leaf growth

Parameter	Tolerant (T)			Sensitive (S)			T+S	ANOVA *P*-values		
	Ctrl	ST	Ctrl versus ST (%)	Ctrl	ST	Ctrl versus ST (%)	Ctrl versus ST (%)	*Treatment*	*Tolerance*	*Treatment* Tolerance*
FLL (cm)	39±9	26±5	–35	28±2	14±1	–51	–41	**0.002**	**0.0066**	0.897
T_{LE} (d)*	6.7±0.8 ^{c}	14.4±0.3 ^{a}	116	6.7±0.5 ^{c}	12.1±1.0 ^{b}	80	98	<0.0001	0.0275	**0.0214**
LER (mm h^{-1})	3.29±0.67	0.84±0.14	–74	2.59±0.12	0.55±0.01	–79	–76	**<0.0001**	**0.0373**	0.3341
l_{mat} (µm)	76±6	59±8	–22	75±9	54±3	–28	–25	**0.0016**	0.5554	0.5981
P (cells h^{-1})	42±6	14±1	–65	35±2	11±1	–68	–67	**<0.0001**	**0.0204**	0.3697
D (cells cells^{-1} h^{-1})	0.076±0.015	0.039±0.008	–49	0.081±0.029	0.032±0.007	–61	–55	**0.0022**	0.9341	0.5567
T_c (h)	9.5±1.6	19.7±3.1	108	9.5±3.4	23.8±4.9	151	129	**0.0003**	0.3245	0.3273
N_{div} (cells)	566±106	404±69	–29	474±171	373±59	–21	NS	0.0731	0.3639	0.6443
T_{div} (h)	87±17	171±32	97	85±35	205±46	141	119	**0.0008**	0.4439	0.395
T_{el} (h)	16.59±2.46	55.35±8.62	234	18.97±1.93	52.63±2.31	177	204	**<0.0001**	0.9522	0.377
RER (µm µm^{-1} h^{-1})	0.10±0.01	0.03±0.00	–69	0.09±0.02	0.03±0.00	–66	–68	**<0.0001**	0.5697	0.4611
l_{div} (µm)	15±3	11±1	–24	14±4	12±2	–17	NS	0.0809	0.9554	0.7143
L_{mer} (mm)	5.8±0.9	4.3±0.9	–26	4.4±0.5	3.9±0.4	–13	–20	**0.0274**	**0.0463**	0.2633
L_{el} (mm)	26±5	20±5	–21	23±1	15±1	–35	–28	**0.0106**	0.0601	0.5377
L_{gr} (mm)	32±5	25±6	–22	27±1	19±1	–32	–26	**0.0064**	**0.0358**	0.7023
N_{el} (cells)	700±186	790±118	13	671±105	564±55	–16	NS	0.9068	0.1149	0.2082
N_{gr} (cells)	1266±229	1194±184	–6	1145±245	937±92	–18	NS	0.252	0.1347	0.5647

ST, suboptimal temperatures; FLL, final leaf length; T_{LE}, duration of leaf growth; LER, leaf elongation rate; l_{mat}, mature cell length; P, cell production rate; D, cell division rate; T_C, cell cycle duration; N_{div}, number of cells in the meristem; T_{div}, transit time in the meristem; T_{el}, transit time in elongation zone; RER, relative expansion rate; l_{div}, length of the cells leaving the meristem; L_{mer}, length of the meristem; L_{el}, length of the elongation zone; L_{gr}, length of the growth zone; N_{el}, number of cells in the elongation zone; N_{gr}, number of cells in the growth zone; NS, not significant. Data are means ±SD for three cultivars grown in control and suboptimal temperatures. For each cultivar, n=23 for LER, n=10 for FLL, and n=5 for the rest of the parameters. Percentage change of ST over control (optimal temperatures) data is shown for T and S cultivars, and for all cultivars (T+S) for an overall analysis. *For T_{LE}, a post-hoc Tukey test was done. Data means with the same letter are not significantly different (P>0.05).

51%, whereas in the tolerant lines this reduction was only 35%. These differences were partially explained by differences in leaf elongation rate, which decreased by 74% in the tolerant cultivars and 79% in the sensitive varieties. To compensate for the reduced leaf elongation rates, tolerant lines had an increased duration of leaf growth significantly greater than that of sensitive cultivars (interaction factor, Table 1). The extended growth could potentially be explained by the thermal time theory, which expresses developmental progress as a function of an integrated temperature sum above a base temperature (Ben-Haj-Salah and Tardieu, 1995). Based on thermal time, the duration of leaf growth was reduced by suboptimal temperature, and more strongly in the sensitive than in the tolerant cultivars (Table 2).

Proteome profiling

To investigate the most prominent molecular differences determining tolerance, we performed a proteome analysis related to the inhibition of cell division and expansion in the meristem and elongation zone, respectively. We used tandem mass tag (iTRAQ) semi-quantitative proteomics to compare two selected cultivars, one sensitive (IR50) and the other tolerant (Koshihikari), treatments (control and suboptimal temperatures), and zones (meristem and elongation zone). In total, we identified 559 and 542 proteins for IR50 and Koshihikari, respectively (Supplementary Table S4). Although most of the proteins were shared across zones and treatments in both cultivars (Fig. 2), some were exclusively present in the meristem (8 and 11 for IR50 and Koshihikari, respectively) or in the elongation zone (43 and 48 for IR50 and Koshihikari, respectively). A two-way ANOVA showed a larger number of differentially expressed proteins between zones (210 and 163 for IR50 and Koshihikari, respectively) than in response to stress (68 and 96 proteins significant for treatment or treatment×zone in IR50 and Koshihikari, respectively; Supplementary Table S4). To group proteins with similar expression patterns, we performed a hierarchical clustering of all proteins that had a significant difference for treatment, zone, or treatment×zone effect (Fig. 3). In order to identify the processes overrepresented in the protein profiles in the different clusters, we performed an enrichment analysis.

The global expression profile of the two cultivars was similar (Fig. 3A, B, Supplementary Table S4). In both cultivars there was a cluster with proteins that were most abundant in meristem, enriched for ribosomal and spliceosome proteins (Cluster 1), reflecting the active transcription/translation occurring in proliferating tissues. Both lines also shared a cluster of proteins that were up-regulated in the elongation zone (Cluster 2). This cluster was significantly larger in IR50, and was enriched for photosynthesis and chloroplast in both lines, and also for redox homeostasis in IR50. A third cluster contained proteins that

Table 2. Effect of suboptimal temperatures on the duration of leaf elongation expressed as thermal time

	T		S		ANOVA *P*-values		
	Ctrl	ST	Ctrl	ST	*Treatment*	*Tolerance*	*Treatment*Tolerance*
GDD to achieve FLL (h)	106.7 ^{a}±13.4	100.8 ^{a}±1.9	107.7 ^{a}±7.2	**84.7 ^{b}±7.3**	**<0.0001**	**0.0012**	**0.0002**

T, tolerant; S, sensitive; Ctrl, optimal temperature, ST, suboptimal temperature; GGD. growing degree days; FLL, final leaf length. Data are mean ±SD (n=3) in Ctrl and ST temperatures. A post-hoc Tukey test was done; different letters indicate significantly different values (P<0.05).

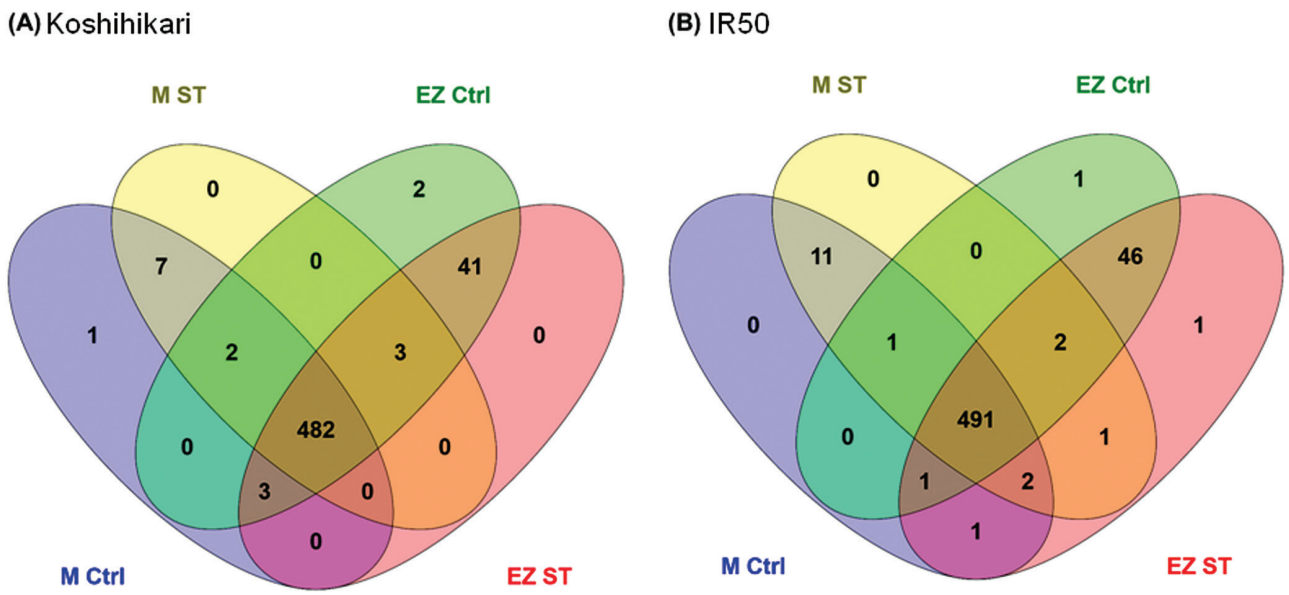

Fig. 2. Distribution of the identified proteins across developmental zones and treatments. Proteomes of (A) Koshihikari and (B) IR50. Samples are marked by zone (M, meristem; EZ, elongation zone) and treatment (Ctrl, optimal temperatures; ST, suboptimal temperatures). (This figure is available in colour at *JXB* online.)

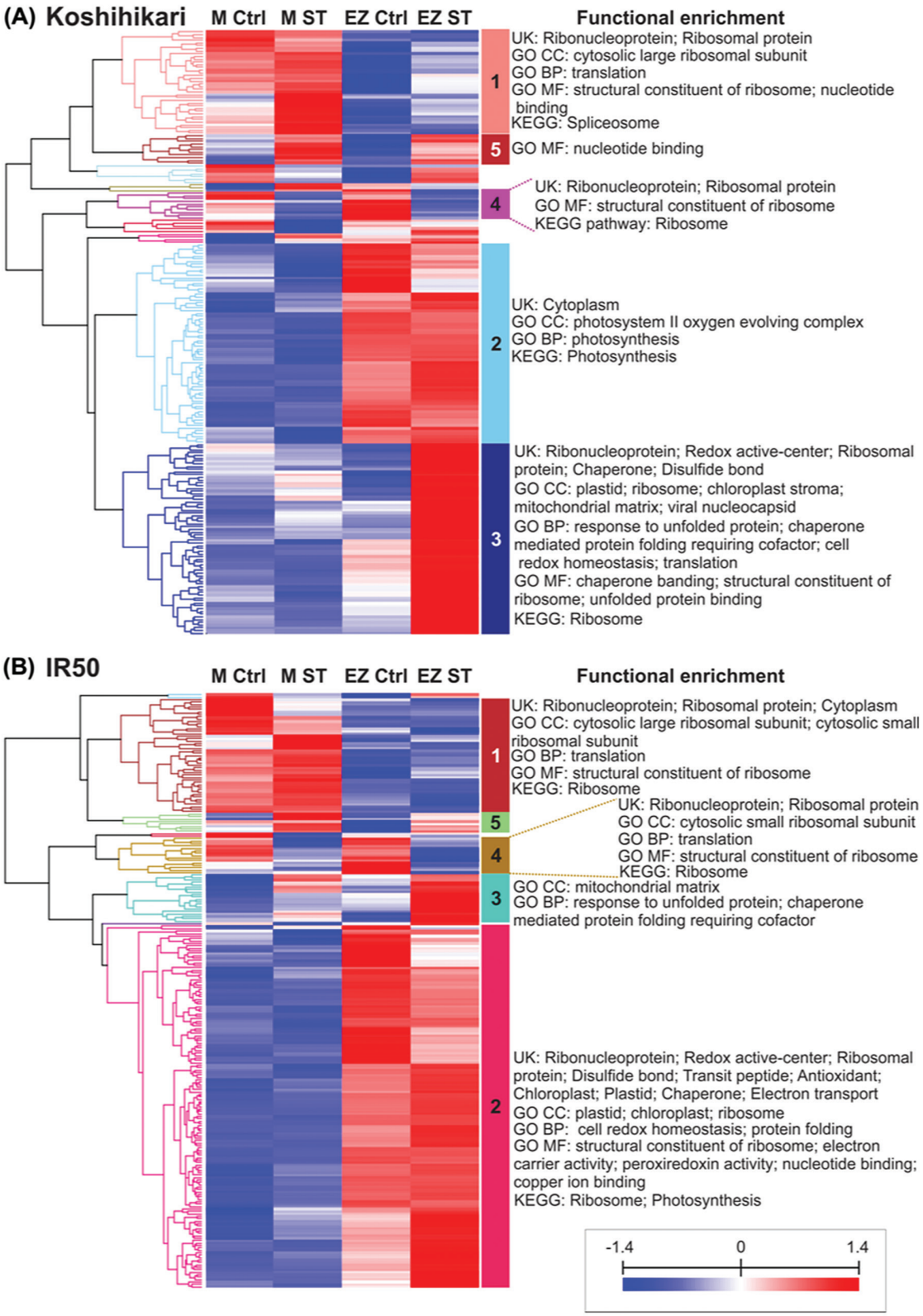

Fig. 3. Hierarchical clustering of differentially expressed proteins. (A) Koshihikari proteins, distance threshold of 1.55; (B) IR50 proteins, distance threshold of 1.57. Treatments are means of three samples and are labelled by zone (M, meristem; EZ, elongation zone) and treatment (Ctrl: optimal temperatures; ST: suboptimal temperatures). The scale at the bottom of the figure represents the abundance of proteins after normalization with *Z*-scoring across rows for the heatmap. Significantly enriched annotation terms are indicated for each cluster. Functional enrichment categories are: Gene Ontology (GO) Biological Processes (GO BP), GO Molecular Function (GO MF), GO Cellular Component (GO CC), KEGG pathways (KEGG), and UniProt Keywords (UK). (This figure is available in colour at *JXB* online.)

were specifically up-regulated by suboptimal temperature in the elongation zone (Cluster 3). This cluster was much larger in Koshihikari, and was enriched for response to unfolded proteins in both lines. It was significantly enriched for redox homeostasis only in Koshihikari (peroxiredoxin, thioredoxin, SOD, and glutaredoxin; Supplementary Table S4), suggesting a link to the tolerance of this line. Both lines also contained a cluster of proteins down-regulated in suboptimal temperatures in both zones (Cluster 4), which was enriched for ribosomal parts, suggesting a general down-regulation of protein synthesis in response to suboptimal temperatures. A cluster of proteins up-regulated by suboptimal temperatures in both zones (Cluster 5), enriched in nucleotide binding, was also present in both cultivars.

Redox metabolites and biochemical analyses

Because the proteome analysis linked redox homeostasis with cold tolerance, we analysed the effect of the treatments on redox state in the leaf growth zone of the cultivars IR50 and Koshihikari.

To determine the levels of reactive oxygen species (ROS), we measured H_2O_2. Under control conditions, H_2O_2 levels were higher towards the base of the leaf and higher in the sensitive line IR50 (Fig. 4A, Supplementary Table S6). In response to suboptimal temperatures, H_2O_2 concentrations increased in all zones, particularly in the two most basal regions. Interestingly, this increase was much stronger in the sensitive cultivar than in the tolerant cultivar Koshihikari.

To assess whether increased ROS levels resulted in oxidative damage, we measured the amount of lipid peroxidation by using MDA as a marker (Shulaev and Oliver, 2006). Consistent with the higher sensitivity and ROS levels, the level of MDA in IR50 increased more than in Koshihikari in response to suboptimal temperatures, particularly in the transition zone between elongating and mature tissues (Fig. 4B, Supplementary Table S6).

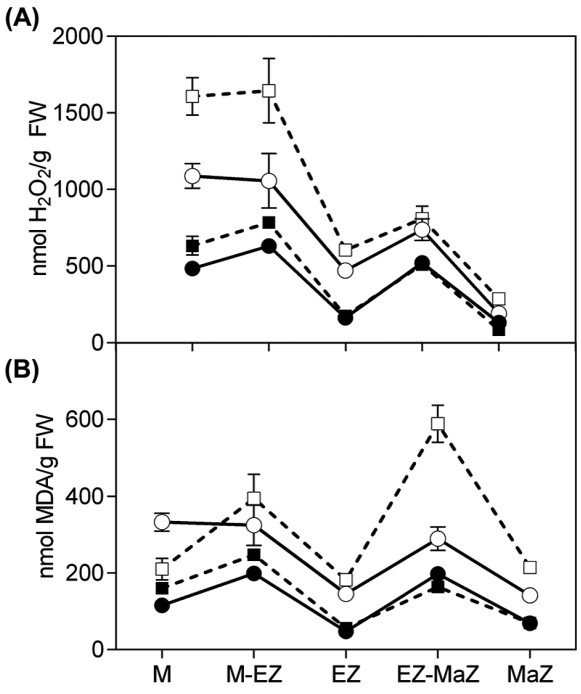

Fig. 4. Effect of suboptimal temperatures on ROS levels and oxidative damage in the growth zone of rice cultivars IR50 (sensitive) and Koshihikari (tolerant). (A) H_2O_2; (B) malondialdehyde (MDA). Ctrl, optimal conditions; ST, suboptimal temperatures; M, meristem; M-EZ, transition zone between the meristem and the elongation zone; EZ, elongation zone; EZ-MaZ, transition zone between EZ and the mature zone; MaZ, mature zone. Data are mean ±SE (n=3).

To test the hypothesis that the higher tolerance of Koshihikari was related to its ability to up-regulate the antioxidant system, we first determined total non-enzymatic antioxidant capacity as FRAP (Benzie and Strain, 1996). Suboptimal temperatures increased FRAP levels towards the mature part of the leaf, and this increase was stronger in Koshihikari than the sensitive cultivar IR50 (Fig. 5A, Supplementary Table S6). The total amount of polyphenols, a powerful non-enzymatic antioxidant (Sharma *et al.*, 2012), also decreased along the growth zone from meristem to mature zone in both cultivars. Low temperatures increased the level of polyphenols in Koshihikari across the growth zone, while in IR50 polyphenols increased only in the elongation zone (Fig. 5B, Supplementary Table S6).

To investigate the potential role of ASC and GSH in the cold response, we determined the relationship between their reduced (ASC, GSH) and total (tASC, tGSH) pools. In control conditions, around 80% of the pools were in the reduced form throughout the growth zone. In suboptimal temperatures, the ASC and GSH pools sere strongly oxidized in the basal regions of the leaves of IR50, while there was relatively little change in Koshihikari leaves (Fig. 5C, D, Supplementary Table S6).

We also assessed the activity of antioxidant enzymes across the growth zone. Suboptimal temperatures were associated with strong increases in the activities of SOD, catalase, glutathione peroxidase, and peroxidases in the basal regions of Koshihikari, but not in IR50 (Fig. 6A–D, Supplementary Table S6). The ASC–GSH cycle is regulated by the activities of APX, monodehydroascorbate reductase, dehydroascorbate reductase, and glutathione reductase. Given the effects of suboptimal temperatures on the oxidative state of these metabolites, particularly in the sensitive cultivar IR50, we measured the activity of these enzymes (Fig. 6, Supplementary Table S6). APX activity was up-regulated in response to the stress in the basal regions of Koshihikari, but not in IR50 (Fig. 6E). Suboptimal temperatures specifically induced monodehydroascorbate reductase activity in the transition zone between elongating and mature tissues and in the mature zone of Koshihikari (Fig. 6F). Under control conditions, dehydroascorbate reductase activities were lower in Koshihikari than in IR50, whereas under suboptimal temperatures they were similar in the two lines (Fig. 6G). Glutathione reductase, glutaredoxin, and thioredoxin were all up-regulated by suboptimal temperatures only in Koshihikari (Fig. 6H–J). These up-regulated enzyme activities correlate closely with the overrepresentation of antioxidant proteins among the up-regulated proteins in the tolerant line and with the ability of this line to maintain the oxidation state of ASC and GSH under suboptimal temperatures.

Discussion

Our study identified differences in leaf growth regulation between cultivars with contrasting tolerance to suboptimal temperatures. In accordance with our previous results (Gazquez

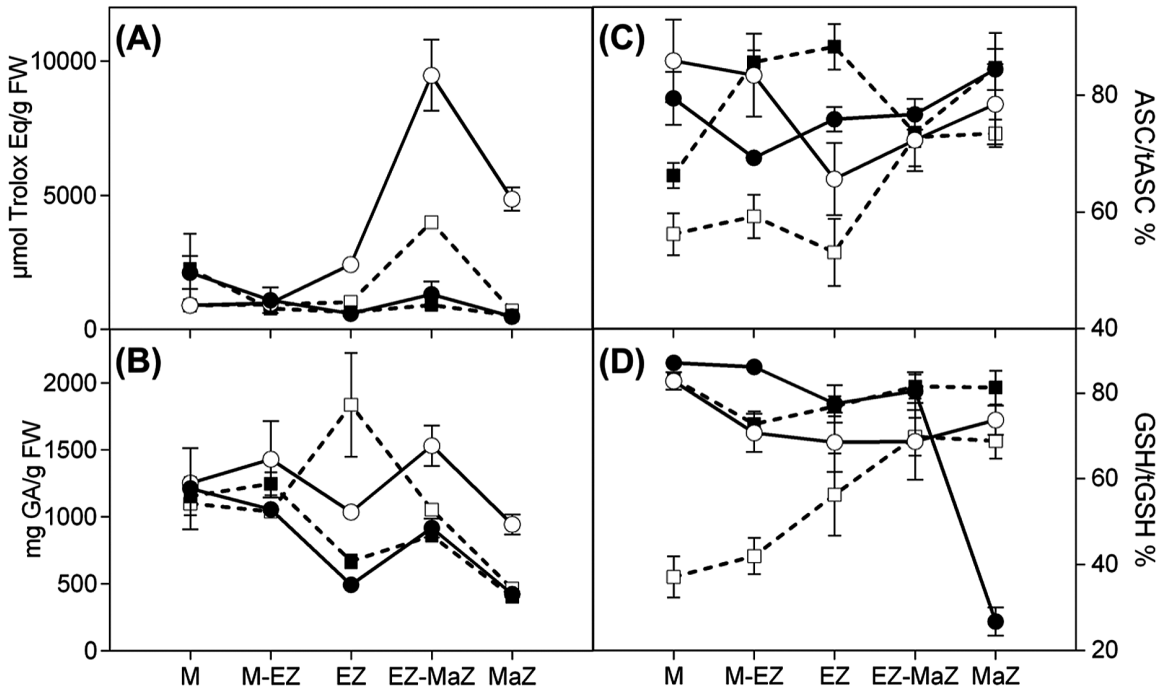

Fig. 5. Effect of suboptimal temperatures on levels of non-enzymatic antioxidants in the growth zone of rice cultivars IR50 (sensitive) and Koshihikari (tolerant). (A) Ferric reducing ability of plasma (FRAP); (B) polyphenol contents as equivalents of gallic acid (GA); (C) reduced ascorbate (ASC) relative to total ascorbate (tASC); (D) reduced glutathione (GSH) relative to total glutathione (tGSH). Ctrl, optimal conditions; ST, suboptimal temperatures; M, meristem; M-EZ, transition zone between the meristem and the elongation zone; EZ, elongation zone; EZ-MaZ, transition zone between EZ and the mature zone; MaZ, mature zone. Data are mean ±SE (n=3).

et al., 2015), the final length of the fourth leaf was reduced to a greater extent in sensitive cultivars than in tolerant cultivars. This difference in length was mainly due to differences in the cultivars' capacity to increase the duration of growth in suboptimal temperatures. The kinematic analysis showed that a reduced cell production, due to a lower cell division rate, was the primary cause of the reduction in growth rate in response to suboptimal temperatures. The effect on cell production was stronger in the sensitive cultivars. Although relative expansion rates were strongly reduced, this was largely compensated by an increase in the period during which cells continue to elongate. Similar results have been found in maize leaves subjected to cold stress (Rymen *et al.*, 2007).

The compensation of a lower leaf elongation rate by an increased duration of growth in response to cold and drought has also been shown for maize (Bos *et al.*, 2000; Avramova *et al.*, 2015). This compensation is particularly strong in response to cold, which caused similar reductions in leaf elongation rate (–70%) but a greater increase in growth duration (+156%) compared with water deficit (–56% and +44%, respectively; Youssef *et al.*, 2016). This led us to hypothesize that the rate of development is slowed more by low temperatures than other stresses. Thermal time models the impact of temperature on plant development (Granier and Tardieu, 1998; Granier *et al.*, 2002; Trudgill *et al.*, 2005) and allowed us to show that, although leaves grow for longer in absolute time, they grow for a shorter thermal period under suboptimal temperatures. In sensitive lines, the reduction of growth duration based on thermal time is larger than in tolerant lines. However, temperature thresholds for varieties adapted to warm climates are higher than for cold-adapted cultivars (Yoshida, 1981; Gao *et al.*, 1992; Trudgill *et al.*, 2005; Counce *et al.*, 2015). Increasing the base temperature in the thermal time calculations reduces the temperature sum required to reach final leaf length and thereby increases the differences between tolerant and sensitive lines even more. This leads us to conclude that cold inhibits developmental duration, particularly in sensitive lines.

The spatial and temporal processes regulating leaf growth are largely independent, implying that the rate and the duration of elongation are subject to different control mechanisms (Nelissen *et al.*, 2016). A recent study of a maize recombinant inbred line (RIL) population linked the duration of growth to the transcriptome of the basal part of the leaf during steady-state growth and found a complex network of genes that were not shared between these parameters (Baute *et al.*, 2015, 2016). RILs that maintained high growth rates for a longer time had a better balance between carbon supply and growth. Hence, it seems that different regulation of the balance between carbon supply and its utilization may explain the difference between the groups (Gazquez *et al.*, 2015, 2018).

Indeed, our proteome analysis supported the involvement of carbon metabolism in cold tolerance. In Koshihikari, up-regulated proteins were overrepresented in the chloroplast structure and stress response classes. In contrast, IR50 showed a down-regulation of proteins from photosystem I (A2YY54 and P0C360; Supplementary Table S4), the oxygen-evolving complex (B8A8L8), and photosystem II (A2YI21 and B8AEM8). Although we and others have demonstrated the inhibition of photosystem II in cold-sensitive lines (Gazquez *et al.*, 2015, 2018) and species (Huner *et al.*, 1998), little is known about photosystem I. Photosystem I is irreversibly affected by stress, and this could cause secondary damage generated by ROS

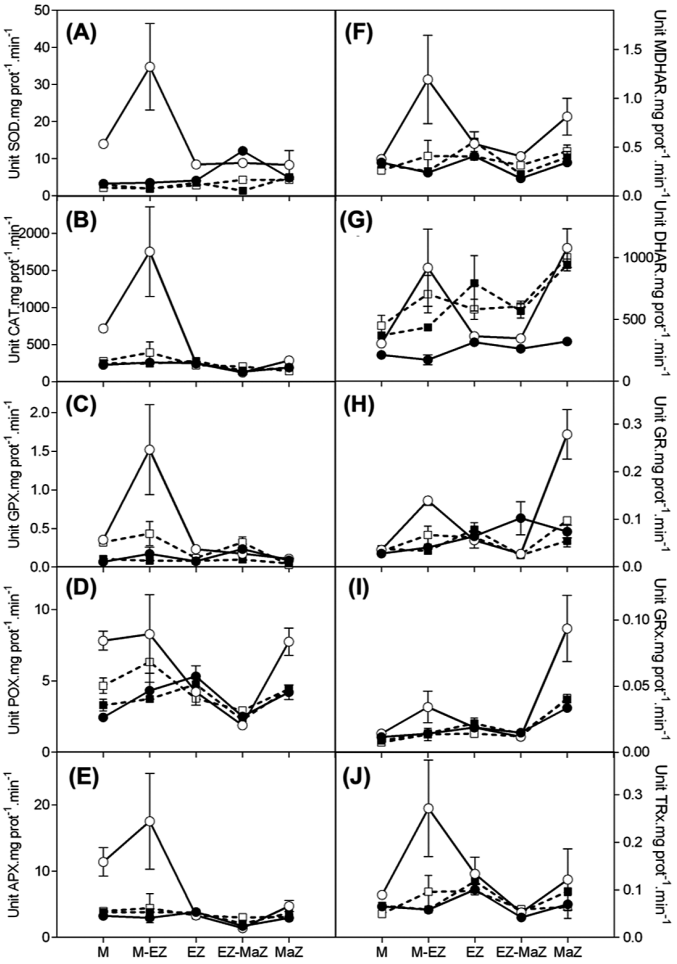

Fig. 6. Effect of suboptimal temperatures on levels of enzymatic antioxidants in the growth zone of rice cultivars IR50 (sensitive) and Koshihikari (tolerant). (A) Superoxide dismutase (SOD), (B) catalase (CAT), (C) glutathione peroxidase (GPX), (D) peroxidases (POX), (E) ascorbate peroxidase (APX), (F) monodehydroascorbate reductase (MDHAR), (G) dehydroascorbate reductase (DHAR), (H) glutathione reductase (GR), (I) glutaredoxins (GRx); (J) thioredoxins (TRx). Ctrl, optimal conditions; ST, suboptimal temperatures; M, meristem; M-EZ, transition zone between the meristem and the elongation zone; EZ, elongation zone; EZ-MaZ, transition zone between EZ and the mature zone; MaZ, mature zone. Data are mean ±SE (n=3).

(Sonoike, 2011). Down-regulation of the oxygen-evolving complex proteins has also been reported in other species subjected to cold (Kosová *et al.*, 2011), and we reported down-regulation at the transcriptome level and confirmed photosystem I damage in the sensitive cultivar IR50 (Gazquez *et al.*, 2018). Carbon balance is determined by photosynthetic and respiration processes (Jacoby *et al.*, 2012). In this regard, the abundance of proteins from the oxidative phosphorylation apparatus in the mitochondria changed in response to suboptimal temperatures. IR50 showed an increased abundance of cytochrome C (A2Y4S9), while in Koshihikari the abundance of this protein decreased (Q0DI31; Supplementary Table S4). Koshihikari also showed a modified abundance of several subunits of cytochrome C oxidase (Q9SXV0, P92683, and Q9SXV0). In photosynthetic tissues, the mitochondria are indispensable for chloroplast function due to the dissipation of excess energy by the respiratory chain, allowing the avoidance of photoinhibition (Noguchi and Yoshida, 2008; Millar *et al.*, 2011; Jacoby *et al.*, 2012). It is therefore significant that proteins from the glycine cleavage system were up-regulated in Koshihikari leaves in response to low temperatures (Q6H713 and A3C6G9). Because Koshihikari did not show a negative effect on the photosystems at the proteome or physiological levels, part of its tolerance to suboptimal temperatures may be the result of the capacity to maintain an active photosynthetic apparatus. However, our proteome analyses enable us to hypothesize that another part of its tolerance may be related to changes in the mitochondria that lead to the protection of its photosynthetic apparatus from ROS damage.

Under stress conditions the reducing power produced by photosynthesis usually exceeds the demand of the Calvin cycle, leading to the generation of ROS, which cause damage (Ensminger *et al.*, 2006; Sharma *et al.*, 2012; You and Chan, 2015). Suboptimal temperatures induced oxidative stress and damage in the growth zone of both cultivars. Although ROS is needed to trigger signalling pathways for both cell division (Livanos *et al.*, 2012) and expansion (Schmidt *et al.*, 2016), a ROS imbalance can cause cell damage.

ROS levels in plants are actively regulated by antioxidant defence mechanisms (Sharma *et al.*, 2012). Koshihikari and IR50 showed different responses of proteins involved in the regulation of redox homeostasis. The non-enzymatic antioxidants accumulated in the elongation and mature zones in particular (Fig. 5A). This finding correlates well with earlier studies showing that the activity of the secondary metabolism increases towards the mature part of the maize leaf (Majeran *et al.*, 2010). ASC and GSH are low-molecular-weight antioxidants that play a key role in the scavenging of ROS. The balance between the reduced and oxidized forms of ASC and GSH are crucial for maintaining cellular redox state (Sharma *et al.*, 2012). While ASC stimulates cell division by mediating the transition to the S-phase, its oxidized form blocks the cell cycle (Potters *et al.*, 2002). Overall, the ASC and GSH redox state was more strongly affected by temperature in the meristem of IR50 than in Koshihikari, and this difference could therefore contribute to the different sensitivities of cell production in the two lines to suboptimal temperature. The enzymes from the ASC–GSH cycle, which control the ratios between the oxidized and reduced forms of these two metabolites, showed a particular increase in activity in the transition zone between the meristem and the elongation zone of Koshihikari, while no major changes were detected in IR50. As the size of the meristem is controlled in this region (Nelissen *et al.*, 2012), this may explain why the meristem size of the sensitive line was reduced twice as much as in the tolerant line. In the stroma, the reduction of monodehydroascorbate to ASC also depends on the availability of the reduced form of ferredoxin and, in turn, in the activity of the stromal subunit of photosystem I (psaC) (Gallie, 2013). Consistently, a ferredoxin was up-regulated in the elongation zone of Koshihikari (A0A0P0W0Z6) in response to suboptimal temperatures, and psaC was down-regulated in IR50.

APX is a major ROS-scavenging enzyme that detoxifies peroxide in plants (Mittler, 2006). From the eight annotated APXs described in *japonica*, *OsAPX1* and *OsAPX2* are found in the cytosol (Teixeira *et al.*, 2006). *Indica* cultivars have two homologs for *OsAPX1* and one for *OsAPX2*. *OsAPX2* was detected in the proteome of both cultivars (Q9FE01 and B8B6B6;

Supplementary Table S4) but the abundance did not change in response to suboptimal temperature, while all homologs of *OsAPX1* (Q10N21, A2XFC7, and A2XFD1) were down-regulated. However, APX activity was up-regulated in the meristem of Koshihikari in response to suboptimal temperature (Fig. 6E), probably as a result of the activity of other APXs.

In contrast to metabolites, the antioxidant enzymes SOD, catalase, glutathione peroxidase, peroxidase, thioredoxin, and glutaredoxin were specifically up-regulated at the base of the leaf in the tolerant line under suboptimal temperatures (Fig. 6). SOD enzymes are the first line of defence against ROS, catalysing the dismutation of superoxide to oxygen and H_2O_2 (Gill and Tuteja, 2010; Sharma *et al.*, 2012; Kaushik and Roychoudhury, 2014). In fact, Koshihikari showed up-regulation of a protein with SOD activity in the elongation zone (Q6ZBZ2; Supplementary Table S4), *OsGLP1*, a cell-wall-associated protein involved in the regulation of plant growth (Banerjee and Maiti, 2010; Banerjee *et al.*, 2010; Dehury *et al.*, 2013). Catalase activity is indispensable for ROS detoxification under stress conditions, since it has a fast turnover (Gill and Tuteja, 2010; Sharma *et al.*, 2012), and it showed the same pattern as SOD (Fig. 6A, B). Glutathione peroxidase and peroxidase constitute large families of enzymes that reduce H_2O_2 and other peroxides, and hence are important for ROS scavenging (Gill and Tuteja, 2010). In accordance, two peroxidases were up-regulated in Koshihikari (Q6ER94 and Q7F8S5). Peroxiredoxins, thioredoxins, and glutaredoxins also play an important role as scavengers of H_2O_2 as an alternative to the water–water cycle (Dietz *et al.*, 2006; Miyake, 2010; Dietz, 2016). In agreement with the measured activities, we found that a chloroplastic thioredoxin was up-regulated in the elongation zone of Koshihikari (Q8S091). However, the thioredoxin *OsTrx23* (Q0D840) was down-regulated but, because it is related to stomatal closure (Ishiwatari *et al.*, 1995, 1998; Zhang *et al.*, 2011), its down-regulation probably explains the increase in stomatal conductance we reported earlier (Gazquez *et al.*, 2015). Regarding glutaredoxin, Koshihikari showed up-regulation of two proteins in both the meristem and elongation zone (P55142 and Q851Y7). Previously, we also found up-regulation of enzymatic antioxidant levels in the meristem of maize leaves in response to drought and demonstrated that overexpression of SOD can stimulate cell division and leaf growth (Avramova *et al.*, 2015).

In both cultivars, proteins related to ribosomes were down-regulated in response to suboptimal temperatures in both the meristem and the elongation zone (Fig. 3, Supplementary Table S4). This down-regulation of the translation machinery complements earlier results from rice (Neilson *et al.*, 2011) and petunia (Zhang *et al.*, 2016) subjected to cold, showing a down-regulation of histone levels. The regulation of chromatin and histones plays a key role in transcriptional regulation in response to environmental stresses, and therefore provides a global stress-response mechanism (Dong *et al.*, 2003; Heidarvand and Maali Amiri, 2010; Kim *et al.*, 2015; Asensi-Fabado *et al.*, 2017). Both cultivars also showed an up-regulation of proteins related to protein folding and chaperonins, demonstrating additional efforts to assure the correct folding of proteins necessary for their function (Wang *et al.*, 2004).

Although oxidative damage occurred in both cultivars, the sensitive cultivar accumulated higher levels of damage. This could be correlated with the stronger up-regulation of antioxidant capacity in Koshihikari compared with IR50. Non-enzymatic antioxidant power was strongly increased in the tolerant cultivar, especially towards the mature part of the leaves. Enzymatic antioxidant power was also up-regulated to protect the proliferating tissue at the base of the leaf. Taken together, the findings of this study directly link tolerance to suboptimal temperatures with the ability to up-regulate both the enzymatic and non-enzymatic antioxidant systems in the growth zone of the leaf.

Supplementary data

Supplementary data are available at *JXB* online.

Table S1. Experimental design of iTRAQ proteome analysis.

Table S2. Peptides detected in the proteome analysis of each pool based on *japonica* and *indica* databases.

Table S3. Peptide abundances after CONSTANd normalization according to *japonica* and *indica* databases.

Table S4. Protein abundances and statistical analyses.

Table S5. Kinematic analysis parameters for the individual cultivars.

Table S6. Three-way ANOVA of the redox parameters.

Fig. S1. The effect of suboptimal temperatures on the length of the developmental zones.

Fig. S2. The effect of suboptimal temperatures on the cell length profile.

Data availability

The MS data have been deposited to the ProteomeXchange Consortium via the PRIDE (Vizcaíno et al., 2016) partner repository with the data set identifier PXD011128 (http://proteomecentral.proteomexchange.org/cgi/GetDataset?ID=PXD011128).

Acknowledgements

AG was supported by the AMIDILA ERASMUS Mundus Action 2 doctoral exchange grant, a CONICET (National Research Council of Argentina) doctoral grant, and a DocPro1 fellowship from the University of Antwerp. HAE was supported by a postdoctoral fellowship from the Flemish Science Foundation (FWO, 12U8918N). We thank Viktoriya Avramova for her assistance with kinematic and proteome analyses.

References

Aebi H. 1984. Catalase in vitro. Methods in Enzymology **105**, 121–126.

Allen DJ, Ort DR. 2001. Impacts of chilling temperatures on photosynthesis in warm-climate plants. Trends in Plant Science **6**, 36–42.

Asensi-Fabado MA, Amtmann A, Perrella G. 2017. Plant responses to abiotic stress: The chromatin context of transcriptional regulation. Biochimica et Biophysica Acta **1860**, 106–122.

Avramova V. 2016. An integrated approach to unravel the growth response of maize leaves to drought. PhD thesis, University of Antwerp.

Avramova V, AbdElgawad H, Vasileva I, Petrova AS, Holek A, Mariën J, Asard H, Beemster GTS. 2017. High antioxidant activity

facilitates maintenance of cell division in leaves of drought tolerant maize hybrids. Frontiers in Plant Science **8**, 84.

Avramova V, AbdElgawad H, Zhang Z, *et al*. 2015. Drought induces distinct growth response, protection, and recovery mechanisms in the maize leaf growth zone. Plant Physiology **169**, 1382–1396.

Banerjee J, Das N, Dey P, Maiti MK. 2010. Transgenically expressed rice germin-like protein1 in tobacco causes hyper-accumulation of H_2O_2 and reinforcement of the cell wall components. Biochemical and Biophysical Research Communications **402**, 637–643.

Banerjee J, Maiti MK. 2010. Functional role of rice germin-like protein1 in regulation of plant height and disease resistance. Biochemical and Biophysical Research Communications **394**, 178–183.

Barkla BJ, Vera-Estrella R, Pantoja O. 2013. Progress and challenges for abiotic stress proteomics of crop plants. Proteomics **13**, 1801–1815.

Baute J, Herman D, Coppens F, De Block J, Slabbinck B, Dell'Acqua M, Pè ME, Maere S, Nelissen H, Inzé D. 2015. Correlation analysis of the transcriptome of growing leaves with mature leaf parameters in a maize RIL population. Genome Biology **16**, 168.

Baute J, Herman D, Coppens F, De Block J, Slabbinck B, Dell'Acqua M, Pè ME, Maere S, Nelissen H, Inzé D. 2016. Combined large-scale phenotyping and transcriptomics in maize reveals a robust growth regulatory network. Plant Physiology **170**, 1848–1867.

Bellincampi D, Dipierro N, Salvi G, Cervone F, De Lorenzo G. 2000. Extracellular H_2O_2 induced by oligogalacturonides is not involved in the inhibition of the auxin-regulated rolB gene expression in tobacco leaf explants. Plant Physiology **122**, 1379–1385.

Ben-Haj-Salah H, Tardieu F. 1995. Temperature affects expansion rate of maize leaves without change in spatial distribution of cell length: analysis of the coordination between cell division and cell expansion. Plant Physiology **109**, 861–870.

Benzie IF, Strain JJ. 1996. The ferric reducing ability of plasma (FRAP) as a measure of "antioxidant power": the FRAP assay. Analytical Biochemistry **239**, 70–76.

Bonhomme R. 2000. Bases and limits to using 'degree day' units. European Journal of Agronomy **13**, 1–10.

Bos HJ, Tijani-Eniola H, Struik PC. 2000. Morphological analysis of leaf growth of maize: responses to temperature and light intensity. NJAS - Wageningen Journal of Life Sciences **48**, 181–198.

Chakraborty A, Bhattacharjee S. 2015. Differential competence of redox-regulatory mechanism under extremes of temperature determines growth performances and cross tolerance in two indica rice cultivars. Journal of Plant Physiology **176**, 65–77.

Clayton S, Neves PC. 2011. Country snapshot: Brazil. Rice Today **10**, 16–17.

Counce PA, Siebenmorgen TJ, Ambardekar AA. 2015. Rice reproductive development stage thermal time and calendar day intervals for six US rice cultivars in the Grand Prairie, Arkansas, over 4 years. Annals of Applied Biology **167**, 262–276.

Cui S, Huang F, Wang J, Ma X, Cheng Y, Liu J. 2005. A proteomic analysis of cold stress responses in rice seedlings. Proteomics **5**, 3162–3172.

Czesnick H, Lenhard M. 2015. Size control in plants—lessons from leaves and flowers. Cold Spring Harbor Perspectives in Biology **7**, a019190.

Dehury B, Sarma K, Sarmah R, *et al*. 2013. In silico analyses of superoxide dismutases (SODs) of rice (*Oryza sativa* L.). Journal of Plant Biochemistry and Biotechnology **22**, 150–156.

Dhindsa R, Plumbdhindsa P, Thorpe T. 1981. Leaf senescence correlated with increased levels of membrane permeability and lipid peroxidation, and decreased levels of superoxide dismutase and catalase. Journal of Experimental Botany **32**, 93–101.

Di Rienzo J, Casanoves F, Balzarini M, Gonzalez L, Tablada M, Robledo C. 2016. InfoStat. Córdoba: Grupo InfoStat, FCA, Universidad Nacional de Córdoba. http://www.infostat.com.ar

Dietz KJ. 2016. Thiol-based peroxidases and ascorbate peroxidases: why plants rely on multiple peroxidase systems in the photosynthesizing chloroplast? Molecules and Cells **39**, 20–25.

Dietz KJ, Jacob S, Oelze ML, Laxa M, Tognetti V, de Miranda SM, Baier M, Finkemeier I. 2006. The function of peroxiredoxins in plant organelle redox metabolism. Journal of Experimental Botany **57**, 1697–1709.

Dong A, Zhu Y, Yu Y, Cao K, Sun C, Shen WH. 2003. Regulation of biosynthesis and intracellular localization of rice and tobacco homologues of nucleosome assembly protein 1. Planta **216**, 561–570.

Du Z, Bramlage W. 1992. Modified thiobarbituric acid assay for measuring lipid oxidation in sugar-rich plant tissue extracts. Journal of Agriculture and Food Chemistry **40**, 1566–1570.

Ensminger I, Busch F, Huner NPA. 2006. Photostasis and cold acclimation: sensing low temperature through photosynthesis. Physiologia Plantarum **126**, 28–44.

Facette MR, Shen Z, Björnsdóttir FR, Briggs SP, Smith LG. 2013. Parallel proteomic and phosphoproteomic analyses of successive stages of maize leaf development. The Plant Cell **25**, 2798–2812.

FAO. 2016. FAOSTAT. Rome: Food and Agriculture Organization of the United Nations Statistics Division. http://faostat3.fao.org/home/E

Fiorani F, Beemster GTS. 2006. Quantitative analyses of cell division in plants. Plant Molecular Biology **60**, 963–979.

Gallie DR. 2013. The role of L-ascorbic acid recycling in responding to environmental stress and in promoting plant growth. Journal of Experimental Botany **64**, 433–443.

Gammulla CG, Pascovici D, Atwell BJ, Haynes PA. 2011. Differential proteomic response of rice (*Oryza sativa*) leaves exposed to high- and low-temperature stress. Proteomics **11**, 2839–2850.

Gao D, Jln Z, Huang Y, Zhang D. 1992. Rice clock model - a computer model to simulate rice development. Agricultural and Forest Meteorology **60**, 1–16.

Gázquez A, Beemster GTS. 2017. What determines organ size differences between species? A meta-analysis of the cellular basis. New Phytologist **215**, 299–308.

Gazquez A, Maiale SJ, Rachoski MM, Vidal A, Ruiz O, Menéndez A, Rodríguez A. 2015. Physiological response of multiple contrasting rice (*Oryza sativa* L.) cultivars to suboptimal temperatures. Journal of Agronomy and Crop Science **201**, 117–127.

Gazquez A, Vilas JM, Colman Lerner JE, Maiale SJ, Calzadilla PI, Menéndez AB, Rodríguez AA. 2018. Rice tolerance to suboptimal low temperatures relies on the maintenance of the photosynthetic capacity. Plant Physiology and Biochemistry **127**, 537–552.

Gill SS, Tuteja N. 2010. Reactive oxygen species and antioxidant machinery in abiotic stress tolerance in crop plants. Plant Physiology and Biochemistry **48**, 909–930.

Gonzalez N, Vanhaeren H, Inzé D. 2012. Leaf size control: complex coordination of cell division and expansion. Trends in Plant Science **17**, 332–340.

Granier C, Massonnet C, Turc O, Muller B, Chenu K, Tardieu F. 2002. Individual leaf development in *Arabidopsis thaliana*: a stable thermal-time-based programme. Annals of Botany **89**, 595–604.

Granier C, Tardieu F. 1998. Is thermal time adequate for expressing the effects of temperature on sunflower leaf development? Plant, Cell and Environment **21**, 695–703.

Grohs M, Marchesan E, Roso R, Silveira Moraes B. 2016. Attenuation of low-temperature stress in rice seedlings. Pesquisa Agropecuária Tropical **46**, 197–205.

Hakeem KR, Chandna R, Ahmad P, Iqbal M, Ozturk M. 2012. Relevance of proteomic investigations in plant abiotic stress physiology. OMICS: A Journal of Integrative Biology **16**, 621–635.

Heidarvand L, Maali Amiri R. 2010. What happens in plant molecular responses to cold stress? Acta Physiologiae Plantarum **32**, 419–431.

Hodges DM, DeLong JM, Forney CF, Prange RK. 1999. Improving the thiobarbituric acid-reactive-substances assay for estimating lipid peroxidation in plant tissues containing anthocyanin and other interfering compounds. Planta **207**, 604–611.

Huang DW, Sherman BT, Lempicki RA. 2009a. Bioinformatics enrichment tools: paths toward the comprehensive functional analysis of large gene lists. Nucleic Acids Research **37**, 1–13.

Huang DW, Sherman BT, Lempicki RA. 2009b. Systematic and integrative analysis of large gene lists using DAVID bioinformatics resources. Nature Protocols **4**, 44–57.

Huner NPA, Öquist G, Sarhan F. 1998. Energy balance and acclimation to light and cold. Trends in Plant Science **3**, 224–230.

Ishiwatari Y, Fujiwara T, McFarland KC, Nemoto K, Hayashi H, Chino M, Lucas WJ. 1998. Rice phloem thioredoxin h has the capacity to

mediate its own cell-to-cell transport through plasmodesmata. Planta **205**, 12–22.

Ishiwatari Y, Honda C, Kawashima I, Nakamura S, Hirano H, Mori S, Fujiwara T, Hayashi H, Chino M. 1995. Thioredoxin h is one of the major proteins in rice phloem sap. Planta **195**, 456–463.

Jacoby RP, Li L, Huang S, Pong Lee C, Millar AH, Taylor NL. 2012. Mitochondrial composition, function and stress response in plants. Journal of Integrative Plant Biology **54**, 887–906.

Kalve S, De Vos D, Beemster GTS. 2014. Leaf development: a cellular perspective. Frontiers in Plant Science **5**, 362.

Kaushik D, Roychoudhury A. 2014. Reactive oxygen species (ROS) and response of antioxidants as ROS-scavengers during environmental stress in plants. Frontiers in Environmental Science **2**, 53.

Kim JM, Sasaki T, Ueda M, Sako K, Seki M. 2015. Chromatin changes in response to drought, salinity, heat, and cold stresses in plants. Frontiers in Plant Science **6**, 114.

Kosová K, Vítámvás P, Prášil IT, Renaut J. 2011. Plant proteome changes under abiotic stress–contribution of proteomics studies to understanding plant stress response. Journal of Proteomics **74**, 1301–1322.

Kuk YI, Shin JS, Burgos NR, Hwang TE, Han O, Cho BH, Jung S, Guh JO. 2003. Antioxidative enzymes offer protection from chilling damage in rice plants. Crop Science **43**, 2109–2117.

Kumar K, Khan P. 1982. Peroxidase and polyphenol oxidase in excised Ragi (Eleusine-Coracana Cv Pr 202) leaves during senescence. Indian Journal of Experimental Biology **20**, 412–416.

Laurance WF, Sayer J, Cassman KG. 2014. Agricultural expansion and its impacts on tropical nature. Trends in Ecology & Evolution **29**, 107–116.

Lazar C, Gatto L, Ferro M, Bruley C, Burger T. 2016. Accounting for the multiple natures of missing values in label-free quantitative proteomics data sets to compare imputation strategies. Journal of Proteome Research **15**, 1116–1125.

Lee J. 1979. Screening methods for cold tolerance at Crop Experiment Station Phytotron and at Chuncheon. Report of a rice cold tolerance workshop. Los Baños: International Rice Research Institute, 77–90.

Livanos P, Apostolakos P, Galatis B. 2012. Plant cell division: ROS homeostasis is required. Plant Signaling & Behavior **7**, 771–778.

Lowry O, Resebgough N, Farr A, Randall R. 1951. Protein measurements with the Folin Phenol reagent. Journal of Biological Chemistry **193**, 265–275.

Lundberg M, Johansson C, Chandra J, Enoksson M, Jacobsson G, Ljung J, Johansson M, Holmgren A. 2001. Cloning and expression of a novel human glutaredoxin (Grx2) with mitochondrial and nuclear isoforms. Journal of Biological Chemistry **276**, 26269–26275.

Luo L, Zhou WQ, Liu P, Li CX, Hou SW. 2012. The development of stomata and other epidermal cells on the rice leaves. Biologia Plantarum **56**, 521–527.

Maes E, Hadiwikarta WW, Mertens I, Baggerman G, Hooyberghs J, Valkenborg D. 2016. CONSTANd: a normalization method for isobaric labeled spectra by constrained optimization. Molecular & Cellular Proteomics **15**, 2779–2790.

Majeran W, Friso G, Ponnala L, *et al*. 2010. Structural and metabolic transitions of C4 leaf development and differentiation defined by microscopy and quantitative proteomics in maize. The Plant Cell **22**, 3509–3542.

Marcon C, Malik WA, Walley JW, Shen Z, Paschold A, Smith LG, Piepho HP, Briggs SP, Hochholdinger F. 2015. A high-resolution tissue-specific proteome and phosphoproteome atlas of maize primary roots reveals functional gradients along the root axes. Plant Physiology **168**, 233–246.

Méchin V, Damerval C, Zivy M. 2007. Total protein extraction with TCA-acetone. Plant Proteomics **355**, 1–8.

Menéndez A, Rodríguez A, Maiale S, Rodríguez Kessler M, Jimenez Bremont J, Ruiz O. 2013. Polyamines contribution to the improvement of crop plants tolerance to abiotic stress. In: Tuteja N, Gill S, eds. Crop improvement under adverse conditions. New York: Springer, 113–136.

Millar AH, Whelan J, Soole KL, Day DA. 2011. Organization and regulation of mitochondrial respiration in plants. Annual Review of Plant Biology **62**, 79–104.

Mittler R. 2006. Abiotic stress, the field environment and stress combination. Trends in Plant Science **11**, 15–19.

Miyake C. 2010. Alternative electron flows (water-water cycle and cyclic electron flow around PSI) in photosynthesis: molecular mechanisms and physiological functions. Plant & Cell Physiology **51**, 1951–1963.

Murshed R, Lopez-Lauri F, Sallanon H. 2008. Microplate quantification of enzymes of the plant ascorbate-glutathione cycle. Analytical Biochemistry **383**, 320–322.

Neilson KA, Mariani M, Haynes PA. 2011. Quantitative proteomic analysis of cold-responsive proteins in rice. Proteomics **11**, 1696–1706.

Nelissen H, Gonzalez N, Inzé D. 2016. Leaf growth in dicots and monocots: so different yet so alike. Current Opinion in Plant Biology **33**, 72–76.

Nelissen H, Rymen B, Jikumaru Y, Demuynck K, Van Lijsebettens M, Kamiya Y, Inzé D, Beemster GTS. 2012. A local maximum in gibberellin levels regulates maize leaf growth by spatial control of cell division. Current Biology **22**, 1183–1187.

Noguchi K, Yoshida K. 2008. Interaction between photosynthesis and respiration in illuminated leaves. Mitochondrion **8**, 87–99.

Pettkó-Szandtner A, Cserháti M, Barrôco RM, Hariharan S, Dudits D, Beemster GTS. 2015. Core cell cycle regulatory genes in rice and their expression profiles across the growth zone of the leaf. Journal of Plant Research **128**, 953–974.

Ponnala L, Wang Y, Sun Q, Van Wijk KJ. 2014. Correlation of mRNA and protein abundance in the developing maize leaf. The Plant Journal **78**, 424–440.

Potters G, De Gara L, Asard H, Horemans N. 2002. Ascorbate and glutathione: guardians of the cell cycle, partners in crime? Plant Physiology and Biochemistry **40**, 537–548.

Potters G, Horemans N, Bellone S, Caubergs RJ, Trost P, Guisez Y, Asard H. 2004. Dehydroascorbate influences the plant cell cycle through a glutathione-independent reduction mechanism. Plant Physiology **134**, 1479–1487.

Quintero C. 2009. Factores limitantes para el crecimiento y productividad del arroz en Entre Ríos, Argentina. PhD Thesis, Universidade da Coruña.

Rymen B, Coppens F, Dhondt S, Fiorani F, Beemster GTS. 2010. Kinematic analysis of cell division and expansion. In: Hennig L, Köhler C, eds. Methods in molecular biology. plant developmental biology: methods in molecular biology. Totowa: Humana Press, 203–227.

Rymen B, Fiorani F, Kartal F, Vandepoele K, Inzé D, Beemster GTS. 2007. Cold nights impair leaf growth and cell cycle progression in maize through transcriptional changes of cell cycle genes. Plant Physiology **143**, 1429–1438.

Sánchez B, Rasmussen A, Porter JR. 2014. Temperatures and the growth and development of maize and rice: a review. Global Change Biology **20**, 408–417.

Schmidt R, Kunkowska AB, Schippers JH. 2016. Role of reactive oxygen species during cell expansion in leaves. Plant Physiology **172**, 2098–2106.

Sharma P, Jha AB, Dubey RS, Pessarakli M. 2012. Reactive oxygen species, oxidative damage, and antioxidative defense mechanism in plants under stressful conditions. Journal of Botany, **2012**, 217037.

Shulaev V, Oliver DJ. 2006. Metabolic and proteomic markers for oxidative stress. New tools for reactive oxygen species research. Plant Physiology **141**, 367–372.

Sonoike K. 2011. Photoinhibition of photosystem I. Physiologia Plantarum **142**, 56–64.

Teixeira FK, Menezes-Benavente L, Galvão VC, Margis R, Margis-Pinheiro M. 2006. Rice ascorbate peroxidase gene family encodes functionally diverse isoforms localized in different subcellular compartments. Planta **224**, 300–314.

Trudgill DL, Honek A, Li D, Van Straalen NM, Straalen NM, Honěk A, Li D, Van Straalen NM. 2005. Thermal time – concepts and utility. Annals of Applied Biology **146**, 1–14.

Tyanova S, Temu T, Sinitcyn P, Carlson A, Hein MY, Geiger T, Mann M, Cox J. 2016. The Perseus computational platform for comprehensive analysis of (prote)omics data. Nature Methods **13**, 731–740.

Vizcaíno JA, Csordas A, del-Toro N, *et al*. 2016. 2016 update of the PRIDE database and its related tools. Nucleic Acids Research **44**, D447–D456.

Wand M, Jones M. 1995. Kernel smoothing. Boca Raton: Chapman & Hall/CRC Press.

Wang W, Chen Q, Hussain S, Mei J, Dong H, Peng S, Huang J, Cui K, Nie L. 2016. Pre-sowing seed treatments in direct-seeded early rice: consequences for emergence, seedling growth and associated metabolic events under chilling stress. Scientific Reports **6**, 19637.

Wang W, Vinocur B, Shoseyov O, Altman A. 2004. Role of plant heat-shock proteins and molecular chaperones in the abiotic stress response. Trends in Plant Science **9**, 244–252.

Wolosiuk RA, Crawford NA, Yee BC, Buchanan BB. 1979. Isolation of three thioredoxins from spinach leaves. Journal of Biological Chemistry **254**, 1627–1632.

Yoshida S. 1981. Fundamentals of rice crop science. Los Baños: International Rice Research Institute.

You J, Chan Z. 2015. ROS regulation during abiotic stress responses in crop plants. Frontiers in Plant Science **6**, 1092.

Youens-Clark K, Buckler E, Casstevens T, *et al*. 2011. Gramene database in 2010: updates and extensions. Nucleic Acids Research **39**, D1085–D1094.

Youssef C, Aubry C, Montrichard F, Beucher D, Juchaux M, Ben C, Prosperi JM, Teulat B. 2016. Cell length instead of cell number becomes the predominant factor contributing to hypocotyl length genotypic differences under abiotic stress in Medicago truncatula. Physiologia Plantarum **156**, 108–124.

Zhang CJ, Zhao BC, Ge WN, Zhang YF, Song Y, Sun DY, Guo Y. 2011. An apoplastic h-type thioredoxin is involved in the stress response through regulation of the apoplastic reactive oxygen species in rice. Plant Physiology **157**, 1884–1899.

Zhang Q, Zhang J, Shen J, Silva A, Dennis DA, Barrow CJ. 2006. A simple 96-well microplate method for estimation of total polyphenol content in seaweeds. Journal of Applied Phycology **18**, 445–450.

Zhang W, Zhang H, Ning L, Li B, Bao M. 2016. Quantitative proteomic analysis provides novel insights into cold stress responses in Petunia seedlings. Frontiers in Plant Science **7**, 1–13.